Top-quark production in hadron-hadron collisions and anomalous top-quark–gluon couplings

P. Haberl, O. Nachtmann, and A. Wilch
Institut für Theoretische Physik, Universität Heidelberg, Philosophenweg 16, D-69120 Heidelberg, Federal Republic of Germany

(Received 1 June 1995; revised manuscript received 15 November 1995)

We discuss the influence of anomalous $t\overline{t}G$ couplings on total and differential $t\overline{t}$ production cross sections in hadron-hadron collisions. We study in detail the effects of a chromoelectric and a chromomagnetic dipole moment d_t' and μ_t' of the top quark. We estimate the values of d_t' and μ_t' which are allowed by the present Fermilab Tevatron experimental results on top-quark production in $p\overline{p}$ collisions. In the μ_t'-d_t' plane, we find a whole region where the anomalous couplings give a zero net contribution to the total top-quark production rate. In differential cross sections, the anomalous moments have to be quite sizable to give measurable effects. A chromoelectric dipole moment of the top quark violates CP invariance. We discuss a CP-odd observable $\hat{O}_L$ which allows for a direct search for CP violation in top-quark production. We find that the presence of a chromomagnetic moment μ_t' can influence the sensitivity of $\hat{O}_L$ to d_t' considerably.

PACS number(s): 14.65.Ha, 13.85.Ni

I. INTRODUCTION

The observation of the top quark has recently been reported by both experimental groups, the Collider Detector at Fermilab (CDF) and D0 Collaborations, working at the Fermilab Tevatron $p\overline{p}$ collider. The latest CDF value for the top-quark mass is $m_t = 176 \pm 8 \pm 10$ GeV [1], while D0 gives the value of $m_t = 199^{+19}_{-21} \pm 22$ GeV [2]. At the Tevatron, top quarks are pair produced in $p\overline{p}$ collisions at a c.m. energy of $\sqrt{s} = 1.8$ TeV. Based on an integrated luminosity of 67 pb^{-1}, the CDF result for the total cross section for this reaction is found to be [1]

$$\sigma_{\text{expt}}(p\overline{p} \to t\overline{t}X) = 6.8^{+3.6}_{-2.4} \text{ pb}. \tag{1}$$

The D0 Collaboration obtains from a data sample corresponding to 50 pb^{-1} the cross section [2]

$$\sigma_{\text{expt}}(p\overline{p} \to t\overline{t}X) = 6.4 \pm 2.2 \text{ pb}. \tag{2}$$

Both central values are higher than the theoretical prediction [3]

$$\sigma_{\text{th}}(p\overline{p} \to t\overline{t}X) = 4.79^{+0.67}_{-0.41} \text{ pb} \quad \text{for } m_t = 176 \text{ GeV}, \tag{3}$$

obtained from a $O(\alpha_s^3)$ standard model (SM) calculation including a resummation of the leading soft gluon corrections to all orders of perturbation theory. The electroweak corrections are known to be small, of the order of a few percent [4]. For higher values of m_t, the theoretical cross section is even lower. Taking the values in Eqs. (1)–(3) literally we obtain for a possible anomalous contribution to the cross section $\Delta\sigma$:

$$\Delta\sigma_{\text{expt}} = \sigma_{\text{expt}}^{\text{mean}} - \sigma_{\text{th}} \pm \sqrt{(\delta\sigma_{\text{expt}}^{\text{mean}})^2 + (\delta\sigma_{\text{th}})^2} \simeq 1.8^{+3.0}_{-2.3} \text{ pb}. \tag{4}$$

Thus the presently available experimental and theoretical information allows a rather large anomalous contribution.

Future experimental runs will increase the number of produced $t\overline{t}$ pairs, allowing the comparison of differential cross sections with theory [5–7]. One will be able to investigate also many other observables, e.g., CP-odd ones. From these measurements one expects to obtain detailed information on the couplings of the top quark. This might provide a further confirmation of the standard model or open a window to new physics.

Of special interest is the study of CP-odd observables in top-quark production and other channels of $p\overline{p}$ collisions [8–14]. For theoretical investigations of CP violation in top-quark production and decay in other contexts we refer to [15–29] and references therein.

In this paper we want to investigate possible effects of anomalous top-quark–gluon couplings on total and differential cross sections of the reaction $p\overline{p} \to t\overline{t}X$. To be specific, we assume the existence of chromoelectric and chromomagnetic top dipole moments, d_t' and μ_t'. Although there are stringent experimental bounds on anomalous contributions to dipole moments of light fermions, it is not unreasonable to expect large anomalous moments for the heavy top quark. One way to generate these couplings is the exchange of Higgs scalars in one-loop diagrams in multi-Higgs-boson extensions of the SM. Since the top-quark–Higgs-boson coupling is proportional to m_t, the effective dipole couplings can be quite sizable.

Here we consider the anomalous couplings d_t' and μ_t' as form factors, which could, in principle, depend on the kinematic variables of the reaction. However, in $p\overline{p}$ collisions at $\sqrt{s} = 1.8$ TeV the $t\overline{t}$ pairs are produced near threshold, where *constant* form factors should be a good approximation. Another way to put it is to consider in the framework of effective Lagrangians an expansion in new coupling terms, ordered by their dimension. The expansion parameter is then $1/\Lambda$, with Λ the scale of new physics. Constant dipole moment form factors d_t' and μ_t' correspond then to the dimension 5 terms (after symmetry breaking [17]), i.e., the terms of order $1/\Lambda$, in the effective Lagrangian.

In the following we will neglect all higher order terms $\sim 1/\Lambda^2$, $1/\Lambda^3, \ldots$ in this effective Lagrangian. In the cross sections for $t\overline{t}$ production such terms contribute at the same order in $1/\Lambda$ as the dipole terms which we keep. However, in order not to have an explosion of new parameters, we restrict ourselves explicitly to the dipole terms. In any case it is common practice by experimentalists to give bounds on new couplings by considering the influence of one or two couplings at a time and setting the rest to zero.

Some effects of the top dipole moments d_t' and μ_t' in the reaction

$$p\bar{p}\rightarrow t\bar{t}X \tag{5}$$

have been investigated previously. In [11], the contribution of both electric and magnetic moments to the matrix element of the parton reactions underlying (5), including final quark polarization, was calculated, but only to first order in the anomalous couplings. The quark spin vectors were then used for the construction of a CP-odd observable. In Ref. [12] the contribution of d_t' to various CP-odd observables was studied. In Ref. [14], total and differential cross sections were computed up to fourth order in μ_t', but for vanishing d_t'.

In the following we want to extend the above analyses and investigate the combined effects of d_t' and μ_t' simultaneously. The outline of our calculation is as follows: We will set the light quark masses to zero and compute the parton processes $q\bar{q}\rightarrow t\bar{t}$ and $GG\rightarrow t\bar{t}$ to leading order (LO) in QCD, i.e., at the tree level, but including the effects of d_t' and μ_t'. Convoluting the parton level results with the parton distribution functions, we evaluate the cross section for $p\bar{p}\rightarrow t\bar{t}X$ which depends now, of course, on d_t' and μ_t': $\sigma(d_t',\mu_t')$. We identify the anomalous cross section (calculated to LO) as

$$\Delta\sigma := \sigma(d_t',\mu_t') - \sigma(0,0). \tag{6}$$

We then add $\Delta\sigma$ to the next to leading order (NLO) SM calculation from Ref. [6]. We note here that higher order QCD effects produce, of course, a chromomagnetic moment form factor. These effects are included in the NLO SM calculation and do not concern us here. Our anomalous moment μ_t' is understood as the *additional* piece in the chromomagnetic moment form factor which may be there due to *new* couplings. Similarly, higher order electroweak corrections in the SM will produce a chromoelectric dipole form factor, which, however, is estimated to be unmeasurably small. Thus a sizable chromoelectric dipole form factor must come from physics beyond the SM.

In [6] it was shown that single top differential cross sections from the full NLO calculation in the SM can well be approximated by a multiplication of the LO standard model result with a constant factor between 1.4 and 1.6. Such a constant factor drops out in normalized differential distributions. Thus the effects of new couplings in differential distributions calculated in LO as described below can hardly be masked by NLO SM effects.

Finally we discuss the sensitivity of the CP-odd observable $\hat{O}_L$ from [12] to the chromoelectric dipole moment d_t'. In Ref. [12], $\hat{O}_L$ was computed for vanishing chromomagnetic moment $\hat{\mu}_t'$ and only to first order in d_t'. Further inputs were a top mass of m_t=130 GeV and the 1984 set of parton distribution functions by Duke and Owens. In addition to updating this old analysis with more timely inputs, we also extend it to the case of nonzero $\hat{\mu}_t'$ and higher orders in $\hat{d}_t'$.

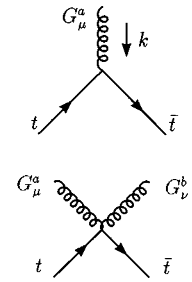

$$-ig_s\frac{\lambda^a}{2}\left[\gamma^\mu + i\frac{\hat{\mu}_t'}{m_t}\sigma^{\mu\nu}k_\nu - \frac{\hat{d}_t'}{m_t}\sigma^{\mu\nu}\gamma_5 k_\nu\right]$$

$$g_s^2 f_{abc}\frac{\lambda^c}{2}\left[i\frac{\hat{\mu}_t'}{m_t}\sigma^{\mu\nu} - \frac{\hat{d}_t'}{m_t}\sigma^{\mu\nu}\gamma_5\right]$$

FIG. 1. Vertex factors following from the top-quark–gluon interaction Lagrangian in Eq. (7). All momenta are taken to be ingoing. The necessity of the second coupling is a consequence of gauge invariance.

II. THE MODEL

We work with the following effective top-quark–gluon interaction Lagrangian:

$$\mathscr{L}_{t\bar{t}G} = -g_s\bar{t}\gamma^\mu G_\mu t - i\,\frac{d_t'}{2}\,\bar{t}\sigma^{\mu\nu}\gamma_5 G_{\mu\nu}t - \frac{\mu_t'}{2}\,\bar{t}\sigma^{\mu\nu}G_{\mu\nu}t. \tag{7}$$

Here g_s is the strong coupling constant, μ_t' and d_t' are the chromomagnetic and chromoelectric dipole moments, $\sigma^{\mu\nu}=(i/2)[\gamma^\mu,\gamma^\nu]$, $G_\mu = G^a_\mu T^a$ with the gluon fields G^a_μ and the $SU(3)_C$ generators $T^a=\frac{1}{2}\lambda^a$ $(a=1,...,8)$, and $G_{\mu\nu}=G^a_{\mu\nu}T^a$ with the gluon field strength tensors $G^a_{\mu\nu}=\partial_\mu G^a_\nu - \partial_\nu G^a_\mu - g_s f_{abc}G^b_\mu G^c_\nu$. Since the anomalous operators have mass dimension 5, we introduce the dimensionless dipole moments $\hat{d}_t'$, $\hat{\mu}_t'$ via

$$d_t' = \frac{g_s}{m_t}\,\hat{d}_t', \quad \mu_t' = \frac{g_s}{m_t}\,\hat{\mu}_t', \tag{8}$$

with the top-quark mass m_t. Both anomalous dipole moment couplings are chirality changing; the magnetic moment term is even under the combined action of charge and parity transformations CP, while the electric moment is CP odd. The signs and factors of 1/2 are chosen such as to yield the correct nonrelativistic limits. In Fig. 1 we show the Feynman vertex factors following from Eq. (7); note in particular that due to gauge invariance there is also a $t\bar{t}GG$ coupling. For the coupling of light quarks q to gluons as well as for the gluon self-coupling we take the SM values.

With this input we calculate the differential cross sections $\hat{\sigma}_{q\bar{q}}$ and $\hat{\sigma}_{GG}$ for the parton level processes

$$q(q_1)+\overline{q}(q_2)\rightarrow t(k_+)+\overline{t}(k_-),$$

$$G(q_1)+G(q_2)\rightarrow t(k_+)+\overline{t}(k_-), \tag{9}$$

to lowest order in QCD, as a function of the usual Mandelstam variables

$$\hat{s}=(q_1+q_2)^2, \quad \hat{t}=(q_1-k_+)^2, \quad \hat{u}=(q_1-k_-)^2. \tag{10}$$

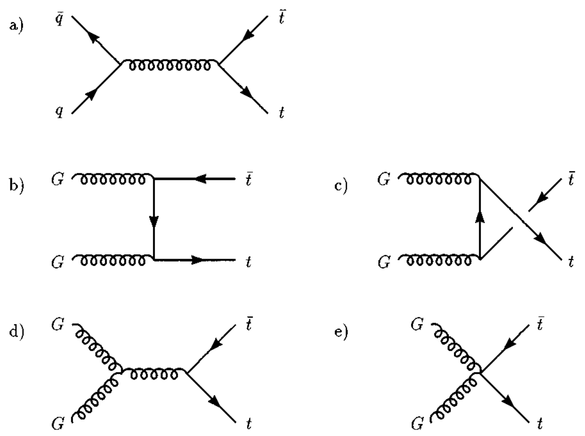

FIG. 2. Feynman diagrams for the quark annihilation $q\overline{q}\to t\overline{t}$ (a) and the gluon fusion $GG\to t\overline{t}$ (b)–(e) processes.

For the quark annihilation, there is only the $\hat{s}$-channel diagram shown in Fig. 2(a) (the corresponding $\hat{t}$- and $\hat{u}$-channel diagrams are absent, since we set the top-quark distribution in the proton and antiproton to zero). The result has the form

$$\frac{d\hat{\sigma}_{q\overline{q}}}{d\hat{t}}=\frac{\pi\alpha_s^2}{\hat{s}^2}\frac{8}{9}\left(\frac{1}{2}-\frac{v-z^2}{4}+2\hat{\mu}_t' +(\hat{\mu}_t'^2-\hat{d}_t'^2)+(\hat{\mu}_t'^2+\hat{d}_t'^2)\frac{v}{z^2}\right), \qquad (11)$$

where we use the abbreviations

$$z=\frac{2m_t}{\sqrt{\hat{s}}}, \quad v=\frac{4}{\hat{s}^2}(\hat{t}-m_t^2)(\hat{u}-m_t^2) \qquad (12)$$

with the kinematical limits $0\leqslant z\leqslant 1$, $z^2\leqslant v\leqslant 1$. The variable v can be expressed in terms of the emission angle $\hat{\vartheta}$ of the top quark in the parton c.m. system as

$$v=1-r^2\cos^2\hat{\vartheta}, \quad r=\sqrt{1-z^2}. \qquad (13)$$

For the gluon fusion process we have to consider the four diagrams in Figs. 2(b)–2(e), and we find

$$\frac{d\hat{\sigma}_{GG}}{d\hat{t}}=\frac{\pi\alpha_s^2}{\hat{s}^2}\frac{1}{12}\left[\frac{1}{2}\left(\frac{16}{v}-9\right)\left(1-\frac{v}{2}+z^2\left(1-\frac{z^2}{v}\right)+4\hat{\mu}_t'(1+\hat{\mu}_t')\right)+4(\hat{\mu}_t'^2+\hat{d}_t'^2)\left(7\frac{1+2\hat{\mu}_t'}{z^2}+\frac{1-5\hat{\mu}_t'}{2v}\right)+4(\hat{\mu}_t'^2+\hat{d}_t'^2)^2\left(\frac{1}{v}-\frac{1}{z^2}+\frac{4v}{z^4}\right)\right]. \qquad (14)$$

In the limit $\hat{d}_t'=\hat{\mu}_t'=0$, we recover the well known SM results [30]. We also checked against Ref. [14] for the case $\hat{d}_t'=0$, where we disagree partly.[1] At Tevatron energies, tops are produced predominantly via the annihilation of quarks; the gluon fusion process becomes important for increasing energy as well as for higher values of the anomalous dipole moments.

According to the parton model, the cross section for the reaction $p\overline{p}\to t\overline{t}X$ is obtained from a convolution of the subprocesses Eq. (9) with parton distribution functions,

$$d\sigma[p(p_1)+\overline{p}(p_2)\to t(k_+)+\overline{t}(k_-)+X(k_X)] =\sum_a\int_0^1 dx_1\int_0^1 dx_2 N_a^p(x_1)N_{\overline{a}}^{\overline{p}}(x_2) \times d\hat{\sigma}_{a\overline{a}}[a(x_1p_1)+\overline{a}(x_2p_2)\to t(k_+)+\overline{t}(k_-)], \qquad (15)$$

where the sum runs over all light quark flavors and the gluons, $a=u,\overline{u},d,\overline{d},c,\overline{c},s,\overline{s},b,\overline{b},G$. We evaluate the distribution functions $N(x,s)$ at the hadron c.m. energy $\sqrt{s}$, whereas the energy $\sqrt{\hat{s}}$ of the parton subprocess sets the scale for α_s. In particular, the total cross section can be written as

$$\sigma(s)=\sum_a\int_0^1 dx_1\int_0^1 dx_2 N_a^p(x_1)N_{\overline{a}}^{\overline{p}}(x_2) \times\Theta(x_1x_2s-4m_t^2)\hat{\sigma}_{a\overline{a}}(\hat{s}=x_1x_2s). \qquad (16)$$

The total parton level cross sections, $\hat{\sigma}_{q\overline{q}}$ and $\hat{\sigma}_{GG}$, can be calculated analytically and we present the result in Appendix A.

Finally we give a useful form of the double differential cross section with respect to rapidity y and transverse energy E_T of the t jet:

$$\frac{d^2\sigma}{dy\,dE_T}=2\sqrt{s}\Delta\sum_a\int_0^1 d\tau\, N_a^p[x_1(\tau)]N_{\overline{a}}^{\overline{p}}[x_2(\tau)] \times[x_1(\tau)x_2(\tau)]^2\frac{d\hat{\sigma}_{a\overline{a}}}{d\hat{t}}, \qquad (17)$$

with

$$\Delta=\frac{\sqrt{s}}{E_T}-2\cosh y, \quad x_1(\tau)=\frac{1}{1+\tau\Delta e^{-y}},$$

$$x_2(\tau)=\frac{1}{1+(1-\tau)\Delta e^{y}}, \qquad (18)$$

and the kinematical limits $m_t\leqslant E_T\leqslant\sqrt{s}/(2\cosh y)$. In $d\hat{\sigma}_{a\overline{a}}/d\hat{t}$ one has to perform the substitutions $\hat{s}\to x_1(\tau)x_2(\tau)s$ and $v\to 4E_T^2/[x_1(\tau)x_2(\tau)s]$.

[1]The formulas given in [14] contain several misprints. In Eq. (2) (quark annihilation) there is a factor of β^2 missing in the last term, as well as an overall factor of 4. In Eq. (6) (gluon fusion) we agree with the terms T_1–T_4, but not with the SM contribution T_0 (in the second factor there is a term $32x^2$ missing). Note also that κ defined in [14] is related to our $\hat{\mu}_t'$ by $\kappa=2\hat{\mu}_t'$.

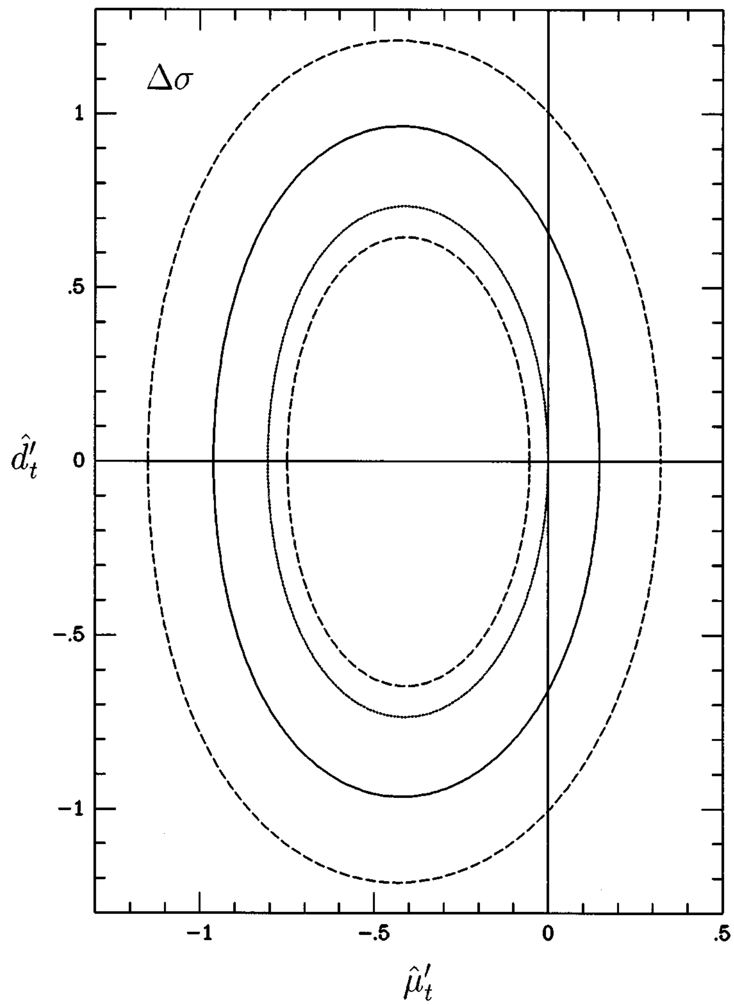

FIG. 3. Contour plot of the anomalous contribution $\Delta\sigma$ defined in Eq. (6) as function of the chromoelectric and chromomagnetic dipole moments $\hat{d}_t'$ and $\hat{\mu}_t'$ [cf. Eq. (8)]. The solid line corresponds to the mean experimental value $\Delta\sigma=1.8$ pb [cf. Eq. (4)]. The dashed lines enclose the experimentally allowed region (1 s.d.): $-0.5\ \mathrm{pb}\leqslant\Delta\sigma\leqslant 4.8$ pb. The dotted line corresponds to the SM result $\Delta\sigma=0$.

III. RESULTS

The numerical evaluation was carried out for the Tevatron; i.e., we considered $p\bar{p}$ collisions at a c.m. energy of $\sqrt{s}=1.8$ TeV. For the top-quark mass we took 175 GeV. We used various parton distribution functions (PDF's) from the CERN library PDFLIB, but found only weak dependence on the actual set; the presented results were computed with the set HO of Glück, Reya, and Vogt [31].

In Fig. 3 we show a contour plot of the anomalous contribution $\Delta\sigma$ defined in Eq. (6) in the $\hat{\mu}_t'$-$\hat{d}_t'$ plane. This quantity has a minimal value of

$$\Delta\sigma_{\min}=-2.00 \quad \text{for } \hat{d}_t'=0,\ \hat{\mu}_t'=-0.4 \tag{19}$$

and increases roughly quadratically with $\hat{d}_t'$, $|\hat{\mu}_t'+0.4|$. We therefore find a whole region where the contributions of $\hat{d}_t'$ and $\hat{\mu}_t'$ cancel. The dashed lines include the experimentally allowed region [cf. Eq. (4)]. Along the solid (dotted) line $\Delta\sigma$ takes the value 1.8 pb (0.0 pb). As explained before, the anomalous contribution has to be added to the theoretical SM value given in Eq. (3). In this way the theoretical value for the total cross section σ could be lowered down to 2.8 pb. More interestingly, we see that the limits on $\Delta\sigma_{\mathrm{expt}}$ in Eq. (4) allow values of the CP violation parameter $\hat{d}_t'$ up to $\hat{d}_t'\approx 1.2$ (at the 1 s.d. level) if $\hat{\mu}_t'$ has an appropriate size.

We have also investigated the dependence of $\Delta\sigma$ on the top-quark mass. For different values of m_t we determined the upper and lower bound including the allowed area (corresponding to the dashed lines in Fig. 3) and the central ring (corresponding to the solid line in Fig. 3). We found that the curves can be very well described by ellipses around centers $(\hat{\mu}_t'/\hat{d}_t')=(c/0)$ with half-axes a and b,

$$\left(\frac{\hat{\mu}_t'-c}{a}\right)^2+\left(\frac{\hat{d}_t'}{b}\right)^2=1. \tag{20}$$

This can easily be understood from the explicit formulas of Appendix A: deviations from an ellipse are due to terms of third or fourth order in $\hat{d}_t'$ and $\hat{\mu}_t'$, which appear only in the subleading gluon fusion process. Moreover, $\Delta\sigma$ can contain

TABLE I. Ellipse parameters a, b, and c parametrizing curves of constant anomalous contribution $\Delta\sigma$, for various values of the top-quark mass [cf. Eq. (20) and Fig. 3].

m_t [GeV]	Upper bound a	Upper bound b	Upper bound c	Central ring a	Central ring b	Central ring c	Lower bound a	Lower bound b	Lower bound c
140	0.125	0.21	−0.379						
160	0.485	0.81	−0.400	0.282	0.51	−0.393			
180	0.805	1.32	−0.425	0.620	1.08	−0.415	0.410	0.77	−0.410
200	1.163	1.87	−0.443	0.945	1.60	−0.435	0.718	1.31	−0.428

only even powers of $\hat{d}_t'$, since it is a CP-even quantity. In Table I we list the parameters a, b, and c for the various ellipses.

The gross feature is that the rings get wider for increasing top-quark mass. In detail we see, for instance, that the upper bound on $|\hat{d}_t'|$ at the 1 s.d. level, leaving $\hat{\mu}_t'$ free, ranges from 0.21 for m_t=140 GeV to 1.87 for m_t=200 GeV. Thus large effects of CP violation due to $\hat{d}_t'$ are not excluded by the present information on σ for this whole range of m_t.

Because of the folding with PDF's differential cross sections get smoothened, but still reflect the characteristic features of the parton level distributions. In Figs. 4–6 we show the normalized differential cross section with respect to the angle ϑ, the emission angle of the t jet in the laboratory ($p\bar{p}$ c.m.) frame. We choose $\vartheta=0$ to correspond to t emission in the direction of flight of the incoming proton. In all three plots, the solid lines are the SM result (in LO). In Fig. 4 we compare this to the distributions obtained with chromoelectric moments $\hat{d}_t'$=0.2, 0.4, 0.6, 0.8, while Fig. 5 shows the effect of a chromomagnetic moment for the values $\hat{\mu}_t'$=0.2, −0.2, −0.4, −0.6. In Fig. 6 we show the angular distributions if both anomalous couplings are nonzero, $(\hat{\mu}_t'/\hat{d}_t')=(-0.4/0.8)$ and $(-0.8/0.4)$. These values are chosen such that the anomalous contribution $\Delta\sigma$ to the total rate would be undetectable (cf. Fig. 3). From Figs. 4–6 we infer that the anomalous couplings would have to be rather large in order to be visible with a limited statistics of $t\bar{t}$ pairs.

In Figs. 7–9 we plot the normalized double differential cross section with respect to rapidity y and transverse momentum p_T of the t jet, as a function of p_T for different values of y. Figure 7 shows the influence of chromoelectric moments $\hat{d}_t'=0.2$ and 0.4; Fig. 8 of chromomagnetic moments $\hat{\mu}_t'=0.2$ and −0.2, compared to the SM result (solid line). In Fig. 9 we show the combined influence of chromoelectric and chromomagnetic moments, again for $(\hat{\mu}_t'/\hat{d}_t')=(-0.4/0.8)$ and $(-0.8/0.4)$. Typically the presence of anomalous dipole moments enhances the production of $t\bar{t}$ pairs with high transverse momentum.

As general feature we observe that normalized differential cross sections are of course more sensitive to anomalous dipole moments than the total rate. For small dipole moments, however, measurable differences occur mainly in phase space regions where the contribution to the total cross section is small, i.e., for large $|\cos\vartheta|$ or large p_T. Only if the anomalous couplings take quite sizable values, one can ex-

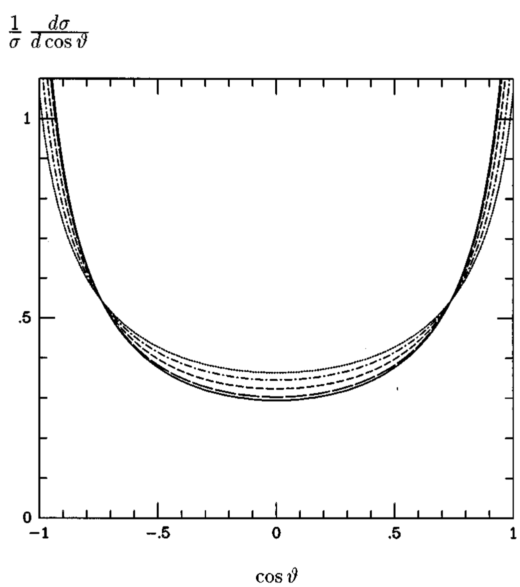

FIG. 4. Normalized differential cross section $(1/\sigma)(d\sigma/d\cos\vartheta)$ for $p\bar{p}\to t\bar{t}X$, where ϑ is the emission angle of the t jet in the $p\bar{p}$ c.m. frame. The solid line represents the LO SM result. The long-dashed (short-dashed, dot-dashed, dotted) line shows the effect of a chromoelectric dipole moment $\hat{d}_t'=0.2$ (0.4, 0.6, 0.8) with $\hat{\mu}_t'=0$.

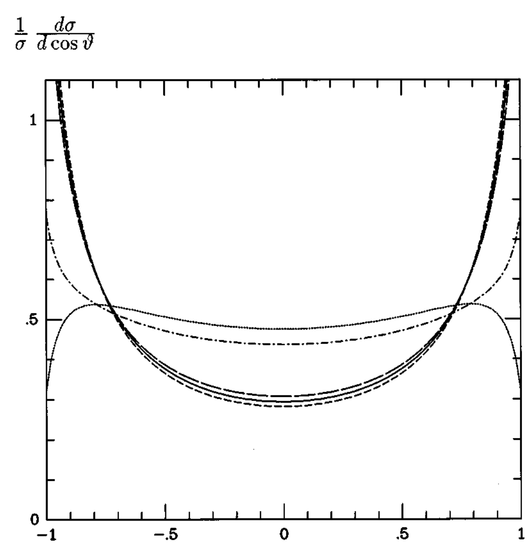

FIG. 5. Same as Fig. 4, now for different values of the chromomagnetic dipole moment. The long-dashed (short-dashed, dot-dashed, dotted) line corresponds to $\hat{\mu}_t'=0.2$ (−0.2, −0.4, −0.6) with $\hat{d}_t'=0$.

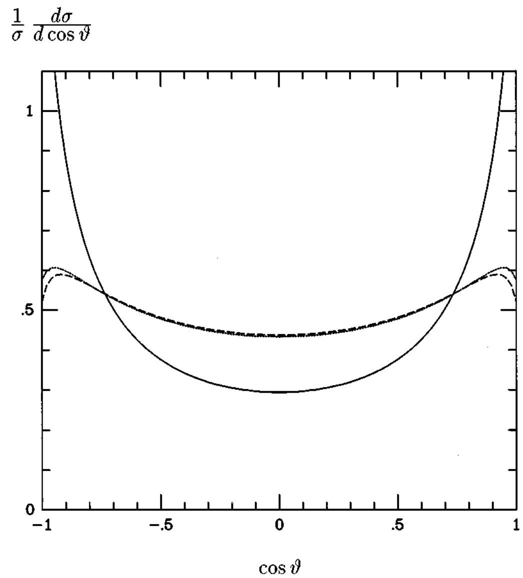

FIG. 6. Same as Fig. 4, with nonzero values for both anomalous dipole moments. The dashed line shows the effect of $(\hat{\mu}_t'/\hat{d}_t')=(-0.4/0.8)$; the dotted line is obtained from $(\hat{\mu}_t'/\hat{d}_t')=(-0.8/0.4)$.

pect clear signals. A shift of the maximum of the curves in Fig. 9 of ≈50 GeV in p_T when going from the SM to $(\hat{\mu}_t'/\hat{d}_t')=(-0.4/0.8)$ or $(-0.8/0.4)$ should clearly be detectable. By a detailed investigation of the $\cos\vartheta$ and y-p_T distributions we found that they are mainly influenced by the chromomagnetic moment $\hat{\mu}_t'$. For fixed $\hat{\mu}_t'$ we found only little dependence on $\hat{d}_t'$ when varying this quantity in the range allowed by the total cross section measurement (Fig. 3).

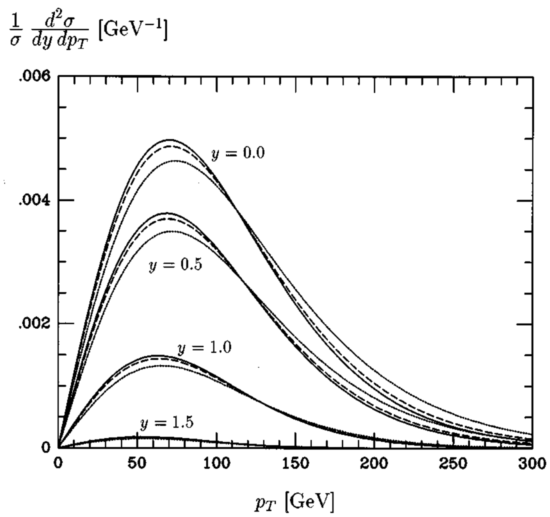

FIG. 7. Normalized double differential cross section $(1/\sigma)(d^2\sigma/dy\,dp_T^2)$ for the reaction $p\overline{p}\rightarrow t\overline{t}\overline{X}$ plotted versus p_T for different values of y. p_T and y are transverse momentum and rapidity of the t jet. Shown is the SM result (solid line) and the distributions obtained with an anomalous chromoelectric moment $\hat{d}_t'=0.2$ (dashed) and $\hat{d}_t'=0.4$ (dotted) for $\hat{\mu}_t'=0$.

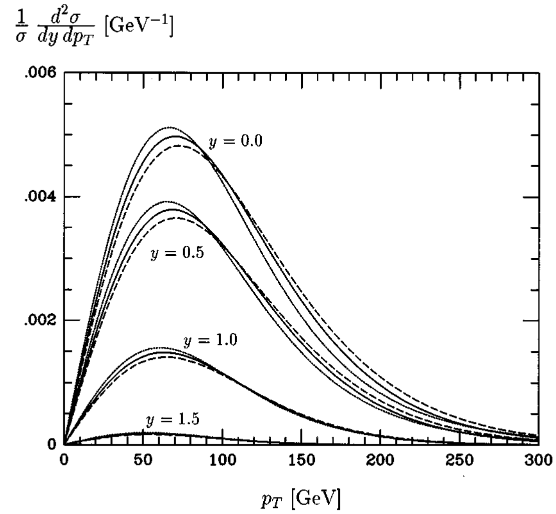

FIG. 8. Same as Fig. 7, now for chromomagnetic dipole moments $\hat{\mu}_t'=0.2$ (dashed) and $\hat{\mu}_t'=-0.2$ (dotted) for $\hat{d}_t'=0$.

IV. A *CP*-ODD OBSERVABLE

In this section we discuss the CP-odd observable $\hat{O}_L$ studied in [12] which is directly sensitive to $\hat{d}_t'$. The observable is constructed for the production and decay sequence

$$
\begin{aligned}
&p+\overline{p}\rightarrow t+\overline{t}+X,\\
&t\rightarrow W^+ + b\rightarrow l^+ + \nu_l + b,\\
&\overline{t}\rightarrow W^- + \overline{b}\rightarrow l^- + \overline{\nu_l} + \overline{b},
\end{aligned} \tag{21}
$$

where $l=e,\mu,\tau$. Let $\mathbf{P}(\mathbf{Q}_+,\mathbf{Q}_-)$ be the momentum of the proton (l^+,l^-) in the $p\overline{p}$ c.m. system. Then $\hat{O}_L$ is defined as

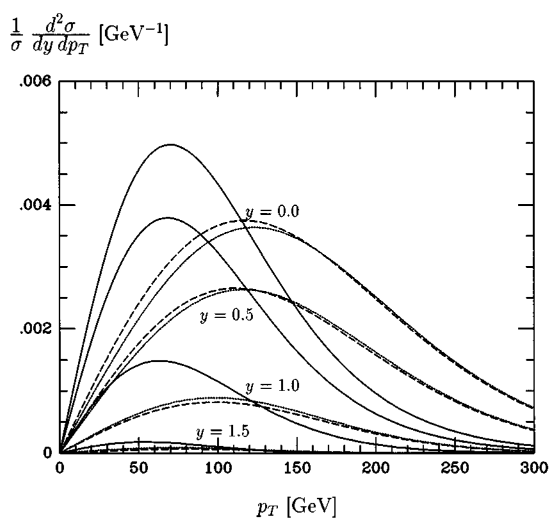

FIG. 9. Same as Fig. 7, now with both $\hat{d}_t'$ and $\hat{\mu}_t'$ nonvanishing. The dashed line corresponds to $(\hat{\mu}_t'/\hat{d}_t')=(-0.4/0.8)$, the dotted line to $(-0.8/0.4)$.

$$\hat{O}_L=\frac{1}{m_t^3|\mathbf{P}|^2}\,\mathbf{P}\cdot(\mathbf{Q}_+\times\mathbf{Q}_-)\mathbf{P}\cdot(\mathbf{Q}_+-\mathbf{Q}_-).\qquad(22)$$

This is an observable of the tensor type T_{ij} introduced in [32] and used in search for CP violation in the decay $Z\to\tau^+\tau^-$ [33]. In [12] the expectation value of $\hat{O}_L$ was calculated for $m_t=130$ GeV keeping only terms of zeroth and first order in $\hat{d}_t'$ and setting $\hat{\mu}_t'=0$, with the result $\langle\hat{O}_L\rangle=-0.012\hat{d}_t'$.

The cross section for reaction (21) is again a convolution of a parton level cross section with parton distribution functions:

$$d\sigma[p(p_1)+\overline{p}(p_2)\to b\overline{b}\overline{l}^+l^-\nu_l\overline{\nu_l}+X]$$
$$=\sum_{a=q,G}\int_0^1 dx_1\int_0^1 dx_2 N_a^p(x_1)N_{\overline{a}}^{\overline{p}}(x_2)$$
$$\times d\hat{\sigma}_{a\overline{a}}[a(x_1p_1)+\overline{a}(x_2p_2)\to b\overline{b}\overline{l}^+l^-\nu_l\overline{\nu_l}].\qquad(23)$$

On parton level we define a density matrix $R^{a\overline{a}}$ for the production process $a\overline{a}\to t\overline{t}$ and two matrices ρ, $\overline{\rho}$ for the decays $t\to l^+\nu_l b$ and $\overline{t}\to l^-\overline{\nu_l}\overline{b}$. The decay processes are computed to leading order in SM couplings only. For the W propagators we take as usual a Breit-Wigner form in the narrow width approximation. The definitions and results[2] for R, ρ, and $\overline{\rho}$ are deferred to Appendix B.

In terms of these density matrices the quantity $d\hat{\sigma}_{a\overline{a}}$ in Eq. (23) takes the form

$$d\hat{\sigma}_{a\overline{a}}(a\overline{a}\to b\overline{b}\overline{l}^+l^-\nu_l\overline{\nu_l})$$
$$=\frac{1}{(8\pi)^{10}}\frac{r}{\hat{s}}\frac{(m_t^2-M_W^2)^2}{m_t^6M_W^2\Gamma_t^2\Gamma_W^2}\,d\Omega_{\hat{\mathbf{k}}_+}d\Omega_{\hat{\mathbf{p}}_+}d\Omega_{\hat{\mathbf{p}}_-}$$
$$\times d\Omega_{\hat{\mathbf{q}}_+}d\Omega_{\hat{\mathbf{q}}_-}\,\mathrm{Tr}[\rho R^{a\overline{a}}\overline{\rho}].\qquad(24)$$

Here M_W and Γ_W are the W mass and width, $\hat{\mathbf{q}}_+(\hat{\mathbf{q}}_-)$ is the $l^+(l^-)$ unit momentum vector in the $W^+(W^-)$ rest system, $\hat{\mathbf{p}}_+(\hat{\mathbf{p}}_-)$ is the $W^+(W^-)$ unit momentum vector in the top-quark (top-antiquark) rest system, $\hat{\mathbf{k}}_+$ is the top-quark unit momentum vector in the parton c.m. system, and $d\Omega_{\hat{\mathbf{q}}_+}(d\Omega_{\hat{\mathbf{q}}_-},\ldots)$ denotes the solid angle element to the unit vector $\hat{\mathbf{q}}_+(\hat{\mathbf{q}}_-,\ldots)$. The expectation values $\langle(\hat{O}_L)^n\rangle$ are defined as

$$\langle(\hat{O}_L)^n\rangle=\frac{\int d\sigma(\hat{O}_L)^n}{\int d\sigma}\quad(n=0,1,2),\qquad(25)$$

where $d\sigma$ is given in (23). To evaluate such integrals we first perform the integrals with the partonic cross section (24). The result for $\int d\hat{\sigma}_{a\overline{a}}\hat{O}_L$ is quite compact, whereas $\int d\hat{\sigma}_{a\overline{a}}\hat{O}_L^2$ consists of several hundreds of terms. In the integral in the denominator of (25), the total partonic cross sections $\int d\hat{\sigma}_{a\overline{a}}$ for the reaction Eq. (21) occur. These can be

[2]The contributions to the CP-odd coefficients $B_5^{a\overline{a}}$ and $B_6^{a\overline{a}}$ (cf. Appendix B) linear in $\hat{d}_t'$ and with $\hat{\mu}_t'=0$ are given in Eqs. (A3) and (A4) of Ref. [12]. In this limit we find full agreement.

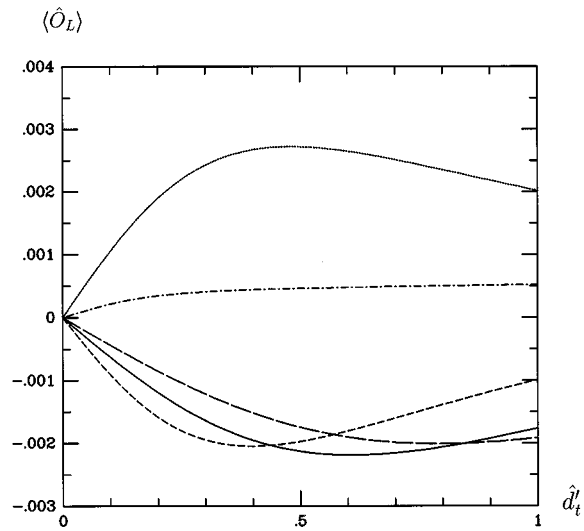

FIG. 10. Expectation value $\langle\hat{O}_L\rangle$ of the CP-odd observable defined in Eq. (22) as function of $\hat{d}_t'$ for $\hat{d}_t'\geqslant 0$. The solid line represents the result for vanishing chromomagnetic moment $\hat{\mu}_t'$, while the long-dashed (short-dashed, dot-dashed, dotted) line shows the influence of $\hat{\mu}_t'=0.2$ $(-0.2, -0.4, -0.6)$. The values of $\langle\hat{O}_L\rangle$ for $\hat{d}_t'<0$ follow from the fact that $\langle\hat{O}_L\rangle$ is an *odd* function of $\hat{d}_t'$.

rewritten in terms of the cross sections for the process $a\overline{a}\to t\overline{t}$ from Appendix A and appropriate branching fractions:

$$\hat{\sigma}_{a\overline{a}}(a\overline{a}\to b\overline{b}\overline{l}^+l^-\nu_l\overline{\nu_l})=B(t\to bW^+)B(W^+\to l^+\nu_l)$$
$$\times B(\overline{t}\to\overline{b}W^-)B(W^-\to l^-\overline{\nu_l})$$
$$\times\hat{\sigma}_{a\overline{a}}(a\overline{a}\to t\overline{t}),\qquad(26)$$

where

$$B(t\to bW^+)=B(\overline{t}\to\overline{b}W^-)=\frac{\alpha_{\rm em}|V_{tb}|^2}{16\sin_W^2}\frac{m_t^2}{M_W^2}\left(1-\frac{M_W^2}{m_t^2}\right)^2\times\left(1+2\frac{M_W^2}{m_t^2}\right)\frac{m_t}{\Gamma_t},$$

$$B(W^+\to l^+\nu_l)=B(W^-\to l^-\overline{\nu_l})=\frac{\alpha_{\rm em}}{12\sin_W^2}\frac{M_W}{\Gamma_W}\qquad(27)$$

with V_{tb} the Cabibbo-Kobayashi-Maskawa matrix element for the t-b transition. Indirect experimental determinations [34] indicate $|V_{tb}|=1$ to a very good approximation. Of course, the convolution of $\int d\hat{\sigma}_{a\overline{a}}(\hat{O}_L)^n$ with the PDF's as indicated in Eq. (23) has to be done numerically.

Our results are summarized in Figs. 10 and 11. In Fig. 10 we display the expectation value $\langle\hat{O}_L\rangle$ as function of $\hat{d}_t'$ for values of the chromomagnetic moment $\hat{\mu}_t'=0.2$, 0.0, -0.2, -0.4, -0.6. We find that the higher terms in $\hat{d}_t'$ cause a deviation from the linear approximation already for moderate values of $\hat{d}_t'$. This deviation consistently lowers the value of $\langle\hat{O}_L\rangle$, i.e., the observable $\hat{O}_L$ gets less sensitive to $\hat{d}_t'$ than expected from the linear approximation [the variance $(\delta\hat{O}_L)^2$

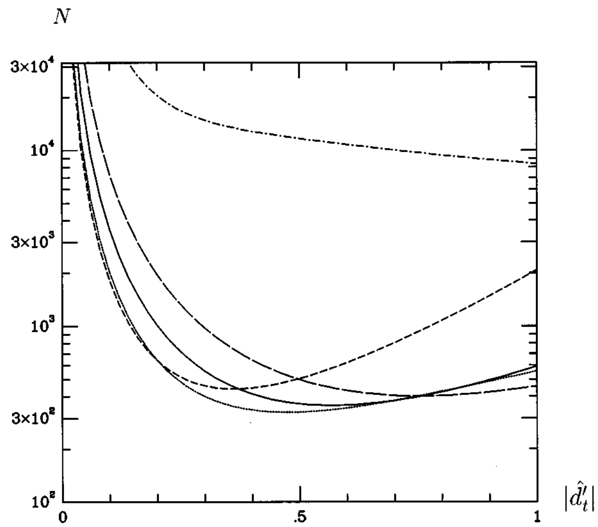

FIG. 11. The number of events N defined in Eq. (31) needed to see a CP violation effect at the 1 s.d. level in the observable $\hat{O}_L$, plotted against the chromoelectric dipole moment $|\hat{d}_t'|$. The solid (long-dashed, short-dashed, dot-dashed, dotted) line corresponds to $\hat{\mu}_t'=0.0$ (0.2, -0.2, -0.4, -0.6).

defined below is almost constant]. If in addition an anomalous chromomagnetic moment of sufficient size is present, the changes are even more drastic. Then $\langle\hat{O}_L\rangle$ can almost vanish ($\hat{\mu}_t'=-0.4$) or even change sign ($\hat{\mu}_t'=-0.6$).

By considering in Fig. 10 the slope of the solid line ($\hat{\mu}_t'=0$) at the origin we can read off our result for the linear approximation. The result $\langle\hat{O}_L\rangle_{\rm lin}=-0.0064\hat{d}_t'$ is only 50% of the value given in Ref. [12], which is mainly due to the higher top-quark mass, whereas the effect of the new PDF's is smaller. To show the effect of the top-quark mass value, we find $\langle\hat{O}_L\rangle_{\rm lin}=-0.0082\hat{d}_t'(-0.0049\hat{d}_t')$ for $m_t=150$ (200) GeV.

In Eq. (21) we have considered the ''diagonal'' reactions with the production of l^- and its antiparticle l^+. Of course, we can also use ''nondiagonal'' reactions where the t and $\bar{t}$ decay to two different lepton flavors l,l':

$$p+\bar{p}\to t+\bar{t}+X,$$

$$t\to W^+ + b\to l^+ + \nu_l + b,$$

$$\bar{t}\to W^- + \bar{b}\to l'^- + \bar{\nu}_{l'} + \bar{b}, \tag{28}$$

and the reaction with $l\leftrightarrow l'$. In this case a nonzero expectation value

$$\frac{1}{2}\langle\hat{O}_L\rangle_{\bar{l}l'}+\frac{1}{2}\langle\hat{O}_L\rangle_{\bar{l}'l}\neq 0 \tag{29}$$

indicates CP violation. With the replacement of expectation values

$$\langle\ \rangle\to\frac{1}{2}\langle\ \rangle_{\bar{l}l'}+\frac{1}{2}\langle\ \rangle_{\bar{l}'l}, \tag{30}$$

all the previous analysis for the ''diagonal'' case applies also to the ''nondiagonal'' one. However, in doing such studies experimentalists must be careful not to introduce any CP bias by cuts, detection efficiencies, etc.

The number of events [Eqs. (21) and (28) taken together] needed to see a 1 s.d. effect can be estimated as

$$N=\left(\frac{\delta\hat{O}_L}{\langle\hat{O}_L\rangle}\right)^2 \tag{31}$$

with the variance

$$(\delta\hat{O}_L)^2=\langle\hat{O}_L^2\rangle-\langle\hat{O}_L\rangle^2. \tag{32}$$

This number N is plotted in Fig. 11 as function of $\hat{d}_t'$, again for the values $\hat{\mu}_t'=0.2$, 0.0, -0.2, -0.4, -0.6. We see that a few thousand events should be sufficient to discover an effect of $|\hat{d}_t'|\gtrsim 0.05$, unless the magnetic moment has a value close to $\hat{\mu}_t'=-0.4$. The contributions of higher order in $\hat{d}_t'$ apparently have the effect that—even for large $\hat{d}_t'$—the minimal number of events to see a 1 s.d. effect is $N_{\rm min}\sim 400$.

V. CONCLUSIONS

In this paper we have investigated the combined effects of a chromoelectric and chromomagnetic dipole moment of the top quark on the reaction $p\bar{p}\to t\bar{t}X$. We have calculated the matrix elements for the parton subprocesses $q\bar{q}\to t\bar{t}$ and $GG\to t\bar{t}$ in leading order QCD. The numerical evaluation of total and differential cross sections was done for Tevatron energies. We have finally presented a detailed analysis of a CP-odd observable.

Our main findings can be summarized as follows.

(1) In the total cross section, a combination of chromoelectric and chromomagnetic dipole moments can yield a positive, negative, or zero contribution. The present experimental information on the total rate allows *substantial* values for the dipole moments: $\hat{d}_t'$, $\hat{\mu}_t'$ of order 1.

(2) Differential distributions can discriminate between chromoelectric and chromomagnetic dipole moments.

(3) The most promising way to disentangle the effects of the two dipole moments is to exploit their different transformation properties under CP. CP-odd observables can only get a nonzero expectation value from a chromoelectric dipole moment $\hat{d}_t'\neq 0$. However, our investigation showed that a nonzero chromomagnetic moment $\hat{\mu}_t'$ can influence the sensitivity of such observables to $\hat{d}_t'$ considerably.

We hope that our formulas and results will be used by experimentalists working at the Tevatron in order to constrain or maybe measure anomalous $t\bar{t}G$ couplings. Anomalous couplings of order 1 could for instance indicate a composite nature of top quarks. We want to end with the historical note that the first indication of the composite nature of the proton was obtained through the measurement of its anomalous magnetic moment [35].

Note added in proof. In the meantime a published version of Ref. [14] has appeared in Phys. Rev. D **52**, 6264 (1995), where all corrections indicated in our footnote 1 have been included. Thus there is now complete agreement of our Eq. (14) for $\hat{d}_t'=0$ with the results of the above paper.

ACKNOWLEDGMENTS

The authors would like to thank W. Bernreuther, A. Brandenburg, and M. Diehl for useful discussions. We also thank T. G. Rizzo for correspondence.

APPENDIX A

In this Appendix we derive the total parton level cross sections $\hat{\sigma}_{a\bar{a}}$, $a=q,G$. With

$$\hat{t}=m_t^2-\frac{\hat{s}}{2}(1-r\cos\hat{\vartheta}),\quad v=-4\left(\frac{\hat{t}}{\hat{s}}-\frac{z^2}{4}\right)\left(1+\frac{\hat{t}}{\hat{s}}-\frac{z^2}{4}\right), \tag{A1}$$

we have

$$\hat{\sigma}_{a\bar{a}}=\int_{-1}^{1}d\cos\hat{\vartheta}\,\frac{d\hat{\sigma}_{a\bar{a}}}{d\cos\hat{\vartheta}}=\int_{\hat{t}_{\rm min}}^{\hat{t}_{\rm max}}d\hat{t}\,\frac{d\hat{\sigma}_{a\bar{a}}}{d\hat{t}}[z,v(\hat{t})], \tag{A2}$$

with $\hat{t}_{\rm min/max}=m_t^2-(\hat{s}/2)(1\pm r)$. One can therefore translate the integration to the simple substitution rules

$$\hat{\sigma}_{a\bar{a}}=r\hat{s}\,\frac{d\hat{\sigma}_{a\bar{a}}}{d\hat{t}}\begin{pmatrix} v\to(2+z^2)/3\\ v^{-1}\to L/2\\ v^{-2}\to(z^{-2}+L/2)/2\end{pmatrix},\quad L=\frac{1}{r}\ln\left(\frac{1+r}{1-r}\right). \tag{A3}$$

These rules can be applied directly to the differential cross sections $d\hat{\sigma}_{a\bar{a}}/d\hat{t}$ of Eqs. (11), (14), leading to the result

$$\hat{\sigma}_{q\bar{q}}=\frac{\pi\alpha_s^2}{\hat{s}}\frac{8r}{27}\left(1+\frac{z^2}{2}+6\hat{\mu}_t'+2(2\hat{\mu}_t'^2-\hat{d}_t'^2)+\frac{2}{z^2}(\hat{\mu}_t'^2+\hat{d}_t'^2)\right), \tag{A4}$$

$$\begin{aligned}\hat{\sigma}_{GG}=\frac{\pi\alpha_s^2}{\hat{s}}\frac{r}{12}\Bigg[&-7-\frac{31}{4}z^2+4L\left(1+z^2+\frac{z^4}{16}\right)\\&+2\hat{\mu}_t'(\hat{\mu}_t'+1)(-9+8L)\\&+(\hat{\mu}_t'^2+\hat{d}_t'^2)\left(\frac{28}{z^2}(1+2\hat{\mu}_t')+L(1-5\hat{\mu}_t')\right)\\&+(\hat{\mu}_t'^2+\hat{d}_t'^2)^2\left(\frac{4}{3z^2}\left(1+\frac{8}{z^2}\right)+2L\right)\Bigg].\end{aligned} \tag{A5}$$

APPENDIX B

The decay matrix ρ for $t\to l^+\nu_l b$ is defined through

$$\begin{aligned}\frac{\pi}{M_W\Gamma_W}\,\delta(p_+^2-M_W^2)\rho_{\alpha'\alpha}&=\sum_{l^+\nu_l b\ \text{spins}}\langle t_{\alpha'}(k_+)|\mathcal{T}|l^+(q_+)\nu_l b\rangle\\&\quad\times\langle l^+(q_+)\nu_l b|\mathcal{T}|t_\alpha(k_+)\rangle,\end{aligned} \tag{B1}$$

where p_+, M_W, and Γ_W are the four-momentum, mass, and width of the intermediate W^+ boson. In our approximation we obtain

$$\rho_{\alpha'\alpha}=\frac{e^4|V_{tb}|^2}{\sin^4\theta_W}\,m_t^2(m_t-2|\mathbf{q}_+'|)[|\mathbf{q}_+'|\delta_{\alpha'\alpha}+\mathbf{q}_{+i}'(\boldsymbol{\sigma}_+{}^i)_{\alpha'\alpha}]. \tag{B2}$$

Here we work in the top-quark rest system, $\mathbf{q}_+'$ is the l^+ momentum, $\boldsymbol{\sigma}_+$ is the vector of Pauli matrices describing the t spin, and α,α' are the t spin indices. The matrix $\bar{\rho}$ for the conjugate decay $\bar{t}\to l^-\bar{\nu}_l\bar{b}$ is obtained from (B2) by the replacements $\mathbf{q}_+'\to-\mathbf{q}_-'$, $\boldsymbol{\sigma}_+\to\boldsymbol{\sigma}_-$.

The production matrix for the partonic process $a\bar{a}\to t\bar{t}$ $(a=q,G)$ is defined as

$$\begin{aligned}R^{a\bar{a}}_{\alpha\beta,\alpha'\beta'}=&\sum_{\substack{a\ \text{spins}\\ \text{and colors}}}\langle t_\alpha(k_+)\bar{t}_\beta(k_-)|\mathcal{T}|a(q_1)\bar{a}(q_2)\rangle\\&\times\langle a(q_1)\bar{a}(q_2)|\mathcal{T}|t_{\alpha'}(k_+)\bar{t}_{\beta'}(k_-)\rangle.\end{aligned} \tag{B3}$$

With the spin vectors $\boldsymbol{\sigma}_+$ and $\boldsymbol{\sigma}_-$ of t and $\bar{t}$ we have the decomposition

$$\begin{aligned}R^{a\bar{a}}_{\alpha\beta,\alpha'\beta'}(\boldsymbol{\sigma}_+,\boldsymbol{\sigma}_-)=&A^{a\bar{a}}\delta_{\alpha\alpha'}\delta_{\beta\beta'}+B^{a\bar{a}}_{ij}(\boldsymbol{\sigma}_+{}^i)_{\alpha\alpha'}(\boldsymbol{\sigma}_-{}^j)_{\beta\beta'}\\&+C^{a\bar{a}}_i(\boldsymbol{\sigma}_+{}^i)_{\alpha\alpha'}\delta_{\beta\beta'}\\&+D^{a\bar{a}}_i\delta_{\alpha\alpha'}(\boldsymbol{\sigma}_-{}^i)_{\beta\beta'}.\end{aligned} \tag{B4}$$

The decomposition of $B^{a\bar{a}}_{ij}$ into symmetric and antisymmetric parts reads

$$\begin{aligned}B^{a\bar{a}}_{ij}=&B^{a\bar{a}}_1\delta_{ij}+B^{a\bar{a}}_2\hat{\mathbf{p}}_i\hat{\mathbf{p}}_j+B^{a\bar{a}}_3\hat{\mathbf{k}}_{+i}\hat{\mathbf{k}}_{+j}+B^{a\bar{a}}_4(\hat{\mathbf{p}}_i\hat{\mathbf{k}}_{+j}+\hat{\mathbf{p}}_j\hat{\mathbf{k}}_{+i})\\&+B^{a\bar{a}}_5\epsilon_{ijl}\hat{\mathbf{p}}_l+B^{a\bar{a}}_6\epsilon_{ijl}\hat{\mathbf{k}}_{+l},\end{aligned} \tag{B5}$$

where $\hat{\mathbf{p}}$ and $\hat{\mathbf{k}}_+$ are the unit vectors of the momenta of proton and top quark in the parton c.m. system. For the quark annihilation process we obtain [$\beta=z^2/v-1$, $\gamma=16/v-9$; for the definition of z and v see Eq. (12)]

$$A^{q\bar{q}}=\frac{4g^4}{9}\left[\left(\frac{1}{2}+\hat{\mu}_t'\right)^2+\frac{v}{2z^2}\beta\left(\frac{z^2}{4}-(\hat{d}_t'^2+\hat{\mu}_t'^2)\right)\right],$$

$$B_1^{q\bar{q}}=\frac{4g^4}{9}\frac{v}{4}\beta\left(\frac{1}{2}+\frac{2}{z^2}(\hat{d}_t'^2-\hat{\mu}_t'^2)\right),$$

$$B_2^{q\bar{q}}=\frac{4g^4}{9}\left(\frac{1}{2}+\hat{\mu}_t'\right)^2,$$

$$B_3^{q\bar{q}}=\frac{4g^4}{9}\frac{1-z}{1+z}\left[\frac{1+z}{2}+\frac{v}{4}\beta-\hat{\mu}_t'\left(\frac{1-v}{z}\right)-\hat{\mu}_t'^2\left(1+\frac{2}{z}+\frac{v}{z^2}\right)\right],$$

$$B_4^{q\bar{q}}=\frac{4g^4}{9}\,(\hat{\mathbf{k}}_+\cdot\hat{\mathbf{p}})\,\frac{1-z}{z}\left[\left(\frac{1}{2}+\hat{\mu}_t'\right)\left(\hat{\mu}_t'-\frac{z}{2}\right)\right],$$

$$B_5^{q\bar{q}}=\frac{4g^4}{9}\,(\hat{\mathbf{k}}_+\cdot\hat{\mathbf{p}})\hat{d}_t'\,\frac{\sqrt{1-z^2}}{z}\left(\frac{1}{2}+\hat{\mu}_t'\right),$$

$$B_6^{q\bar{q}}=\frac{4g^4}{9}\,\hat{d}_t'\,\frac{1}{z}\,\sqrt{\frac{1-z}{1+z}}\left[-\frac{(1+z)^2}{2}-\left(\hat{\mu}_t'-\frac{z}{2}\right)\left(1+\frac{v}{z}\right)\right]. \tag{B6}$$

The production matrix for the gluon fusion process has the coefficients

$$A^{GG}=\frac{g^4}{24}\left[\gamma\left(-\frac{v}{8}-\frac{z^2}{4}\,\beta+\left(\frac{1}{2}+\hat{\mu}_t'\right)^2\right)+(\hat{d}_t'^2+\hat{\mu}_t'^2)\left(\frac{1}{v}\,(1-5\hat{\mu}_t')+\frac{14}{z^2}\,(1+2\hat{\mu}_t')\right)+(\hat{d}_t'^2+\hat{\mu}_t'^2)^2\left(\frac{8v}{z^4}+\frac{2}{z^2}\,\beta\right)\right],$$

$$B_1^{GG}=\frac{g^4}{24}\left[-\gamma\left(\frac{v}{8}+\frac{v}{z^2}\,\hat{d}_t'^2+\left(\frac{z^2}{4}+2\hat{d}_t'^2\right)\beta\right)-\frac{5}{v}\,\hat{\mu}_t'(\hat{d}_t'^2+\hat{\mu}_t'^2)+\frac{1}{v}\,(-7\hat{\mu}_t'-13\hat{\mu}_t'^2+\hat{d}_t'^2)+(\hat{d}_t'^2+\hat{\mu}_t'^2)^2\left(\frac{v}{z^4}+\frac{2}{z^2}\,\beta\right)\right],$$

$$B_2^{GG}=\frac{g^4}{24}\left[-\beta\gamma\left(\frac{1}{2}+\hat{\mu}_t'\right)^2+(\hat{d}_t'^2+\hat{\mu}_t'^2)[(1+\hat{\mu}_t')^2+\hat{d}_t'^2]\left(\frac{1}{z^2}\,\gamma-\frac{16}{v}\left(\frac{2}{v}-1\right)\right)+(\hat{d}_t'^2+\hat{\mu}_t'^2)^2\,\frac{2(1-z^2)}{z^4}\,\beta\right],$$

$$\begin{aligned}B_3^{GG}=\frac{g^4}{24}\,\frac{1-z}{1+z}&\left[-\frac{1}{4}\,\gamma(1+v+2z+\beta(3+4z+2z^2))+\hat{\mu}_t'\left[\frac{7}{v}\,(1+z)+\gamma\left(1+\frac{1}{z}+\beta\left(1+\frac{2-v}{z}\right)\right)\right]\right.\\&+\hat{\mu}_t'^2\gamma\left[1-\frac{1}{z^2}+\frac{2}{z^2}\,\beta\left(v-1+z+\frac{z^2}{2}\right)\right]+(\hat{d}_t'^2+\hat{\mu}_t'^2)\frac{2(1-v)}{vz}+\hat{d}_t'^2\left[-\frac{14}{v}(1+z)-2\gamma\left(\frac{1+z}{v}+\beta-\frac{1-v}{2z^2}\right)\right]\\&+(\hat{d}_t'^2+\hat{\mu}_t'^2)\hat{\mu}_t'\left[-\frac{14}{vz}(1-z)-\frac{14}{z^3}(1+2z)+2\gamma\left(\frac{1}{z^2}-\frac{2}{v}-\frac{v}{z^3}\beta\right)\right]\\&\left.+(\hat{d}_t'^2+\hat{\mu}_t'^2)^2\left[-\frac{14}{vz^2}(1+2z)+\frac{14}{z^4}\left(1+z-\frac{z^2}{2}\right)-\frac{\gamma}{z^2}\left(2\beta+\frac{v}{z^2}\right)\right]\right],\end{aligned}$$

$$\begin{aligned}B_4^{GG}=\frac{g^4}{24}\,(\hat{\mathbf{k}}_+\cdot\hat{\mathbf{p}})(1-z)&\left[\beta\gamma\left(\frac{1}{4}-\frac{1-z}{2z}\,\hat{\mu}_t'-\frac{1}{z}\,\hat{\mu}_t'^2\right)-(\hat{\mu}_t'-2\hat{d}_t'^2)\,\frac{8z}{v^2}\,(1+z)+(\hat{d}_t'^2+\hat{\mu}_t'^2)\left[\frac{2}{z^2}\left(\beta+\frac{1}{2}\right)\gamma-\frac{1-z}{vz}\right]\right.\\&\left.+\hat{\mu}_t'(\hat{d}_t'^2+\hat{\mu}_t'^2)\left[\frac{14}{vz}+\frac{64}{vz^2}\left(\beta+\frac{1}{2}\right)+\frac{9(1-z)}{z^3}\beta\right]+(\hat{d}_t'^2+\hat{\mu}_t'^2)^2\left(\frac{2}{z^2}\left(\beta+\frac{1}{2}\right)\left(\frac{7}{z}+\frac{16}{v}\right)-\frac{2}{z^4}\beta\right)\right],\end{aligned}$$

$$B_5^{GG}=\frac{g^4}{24}\,(\hat{\mathbf{k}}_+\cdot\hat{\mathbf{p}})\hat{d}_t'\frac{\sqrt{1-z^2}}{z}\left[-\frac{32}{v}\left(\beta+\frac{1}{2}\right)\left(\frac{1}{2}+\hat{\mu}_t'^2+\hat{\mu}_t'^2+\hat{d}_t'^2\right)+9\beta\left(\frac{1}{2}+\hat{\mu}_t+\frac{1}{z^2}(\hat{\mu}_t'^2+\hat{d}_t'^2)\right)\right],$$

$$\begin{aligned}B_6^{GG}=\frac{g^4}{24}\,\hat{d}_t'\sqrt{\frac{1-z}{1+z}}&\left[\gamma(1+z)\left(\frac{v}{2z^2}+\beta\right)+\left(\frac{1}{2}+\hat{\mu}_t'\right)\left[\frac{7}{v}\,(z+2)+\gamma\left(\frac{v}{z^2}\,\beta+\frac{2}{z}\left(\beta+\frac{1}{2}\right)\right)\right]\right.\\&\left.+(\hat{d}_t'^2+\hat{\mu}_t'^2)\left[\frac{7}{z^2}\left(\frac{1}{z}\,\beta+2\left(\beta+\frac{1}{2}\right)\right)+\frac{2}{z}\,\gamma\left(\frac{v}{2z^2}+\beta\right)\right]\right].\end{aligned} \tag{B7}$$

The coefficients $C_i^{a\bar{a}}$ and $D_i^{a\bar{a}}$ vanish in both cases. With these explicit expressions we can evaluate the quantity

$$\mathrm{Tr}[\rho R^{a\bar{a}}\bar{\rho}]=\rho_{\alpha'\alpha}R^{a\bar{a}}_{\alpha\beta,\alpha'\beta'}\bar{\rho}_{\beta'\beta} \tag{B8}$$

needed in Eq. (24). The integrations over the W and lepton momenta take their simplest form in the respective rest system of the decaying particle. The observable $\hat{O}_L$ is however defined in terms of proton and lepton momenta $\mathbf{P}$, $\mathbf{Q}_\pm$ in the $p\bar{p}$ c.m. system. Hence we have to perform three boosts on $\hat{O}_L$ (and $\hat{O}_L^2$), which is only possible with the help of an algebraic computer program, for which we took FORM.

[1] CDF Collaboration, F. Abe *et al.*, Phys. Rev. Lett. **74**, 2626 (1995).

[2] D0 Collaboration, S. Abachi *et al.*, Phys. Rev. Lett. **74**, 2632 (1995).

[3] E. Laenen, J. Smith, and W. L. van Neerven, Nucl. Phys. **B369**, 543 (1992); Phys. Lett. B **321**, 254 (1994).

[4] W. Beenakker, A. Denner, W. Hollik, R. Mertig, T. Sack, and D. Wackeroth, Nucl. Phys. **B411**, 343 (1994).

[5] P. Nason, S. Dawson, and R. K. Ellis, Nucl. Phys. **B327**, 49 (1988).

[6] W. Beenakker, W. L. van Neerven, R. Meng, G. A. Schuler, and J. Smith, Nucl. Phys. **B351**, 507 (1991).

[7] S. Frixione, M. L. Mangano, P. Nason, and G. Ridolfi, Phys. Lett. B **351**, 555 (1995); N. Kidonakis and J. Smith, Phys. Rev. D **51**, 6092 (1995).

[8] A. Brandenburg, J. P. Ma, R. Münch, and O. Nachtmann, Z. Phys. C **51**, 225 (1991).

[9] A. Brandenburg, J. P. Ma, and O. Nachtmann, Z. Phys. C **55**, 115 (1992).

[10] C. R. Schmidt and M. Peskin, Phys. Rev. Lett. **69**, 410 (1992).

[11] D. Atwood, A. Aeppli, and A. Soni, Phys. Rev. Lett. **69**, 2754 (1992).

[12] A. Brandenburg and J. P. Ma, Phys. Lett. B **298**, 211 (1993).

[13] T. Arens and L. M. Sehgal, Phys. Lett. B **302**, 501 (1993).

[14] D. Atwood, A. Kagan, and T. G. Rizzo, Report No. SLAC-PUB-6580, 1994 (unpublished).

[15] J. F. Donoghue and G. Valencia, Phys. Rev. Lett. **58**, 451 (1987); **60**, 243(E) (1988).

[16] C. A. Nelson, Phys. Rev. D **41**, 2805 (1990).

[17] W. Bernreuther and O. Nachtmann, Phys. Lett. B **268**, 424 (1991).

[18] J. Körner, J. P. Ma, R. Münch, O. Nachtmann, and R. Schöpf, Z. Phys. C **49**, 447 (1991).

[19] G. L. Kane, G. A. Ladinsky, and C.-P. Yuan, Phys. Rev. D **45**, 124 (1991).

[20] W. Bernreuther, O. Nachtmann, P. Overmann, and T. Schröder, Nucl. Phys. **B388**, 53 (1992).

[21] D. Atwood and A. Soni, Phys. Rev. D **45**, 2405 (1992).

[22] J. P. Ma and A. Brandenburg, Z. Phys. C **56**, 97 (1992).

[23] C. R. Schmidt, Phys. Lett. B **293**, 111 (1992).

[24] W. Bernreuther, P. I. Kemenes, M. Jezabek, J. H. Kühn, B. Lampe, O. Nachtmann, P. Overmann, T. Schröder, J. Steegborn, T. Teubner, and P. M. Zerwas, in e^+e^- *Collisions at 500 GeV: The Physics Potential*, Proceedings of the Workshop, Munich, Annecy, Hamburg, 1991, edited by P. M. Zerwas (DESY Report No. 92-123, Hamburg, 1992).

[25] W. Bernreuther and A. Brandenburg, Phys. Lett. B **314**, 104 (1993); Phys. Rev. D **49**, 4481 (1994).

[26] J. Liu, Phys. Rev. D **47**, R1741 (1993).

[27] B. Grzadkowski, Phys. Lett. B **305**, 384 (1993).

[28] W. Bernreuther and P. Overmann, Z. Phys. C **61**, 599 (1994).

[29] T. Arens and L. M. Sehgal, Nucl. Phys. **B393**, 46 (1993); Phys. Rev. D **50**, 4372 (1994).

[30] M. Glück, J. F. Owens, and E. Reya, Phys. Rev. D **17**, 2324 (1978); B. L. Combridge, Nucl. Phys. **B151**, 429 (1979).

[31] M. Glück, E. Reya, and A. Vogt, Z. Phys. C **53**, 127 (1992); CERN program library PDFLIB.

[32] W. Bernreuther, U. Löw, J. P. Ma, and O. Nachtmann, Z. Phys. C **41**, 143 (1988); **43**, 117 (1989).

[33] OPAL Collaboration, P. D. Acton *et al.*, Phys. Lett. B **281**, 405 (1992); ALEPH Collaboration, D. Buskolic *et al.*, *ibid.* **297**, 459 (1992); OPAL Collaboration, R. Akers *et al.*, Z. Phys. C **66**, 31 (1995).

[34] Particle Data Group, L. Montanet *et al.*, Phys. Rev. D **50**, 1173 (1994).

[35] R. Frisch and O. Stern, Z. Phys. **85**, 4 (1933).